









Interaction of Phytochemicals with Proteins Associated with Mucopolysaccharide Biosynthesis in *Pseudomonas aeruginosa*: a Predictive Study of Biomedical Interest

Luis Moncayo Molina ¹, Diana Carolina Ariás Naravaez ¹, María Verónica Pogyo Morocho ¹, Zandra Maribel Regalado Vazquez ¹, Aleivi Pérez ², María Laura Hurtado-León ³, Carla Lossada ⁴, Lenin González-Paz ^{4,*}

¹ Catholic University of Cuenca, Ecuador; lmoncayom@ucacue.edu.ec, (L.M.M.); diana.arias@ucacue.edu.ec, (D.C.A.N.); marcia.pogyom@ucacue.edu.ec, (M.V.P.M.); zregaladov@ucacue.edu.ec, (Z.M.R.V.);

² University of Zulia. Experimental Faculty of Sciences. General Microbiology Laboratory. Maracaibo-Zulia, Bolivarian Republic of Venezuela; aleiviciencias@gmail.com (A.P.);

³ University of Zulia. Experimental Faculty of Sciences. Maracaibo-Zulia, Bolivarian Republic of Venezuela; marialahurtado@gmail.com (M.L.H.L.);

⁴ Venezuelan Institute for Scientific Research (IVIC). Center for Molecular Biomedicine (CBM). Biocomputation Laboratory (LB). Maracaibo-Zulia, Bolivarian Republic of Venezuela; lossadacarla@gmail.com (C.L.); lgonzalezpaz@gmail.com (L.G.P.)

* Correspondence: lgonzalezpaz@gmail.com (L.G.P.);

Scopus Author ID 6602882448

Received: 22.07.2023; Accepted: 16.11.2023; Published: 17.02.2024

Abstract: *Pseudomonas aeruginosa* is a pathogen that can resist multiple antibiotics and has several ways to cause harm, including the production of biofilms made of mucous exopolysaccharides (EPS). Chronic infections by *P. aeruginosa* are often linked to biofilms associated with the mucoid variant phenotype. A large group of proteins is involved in EPS production in *P. aeruginosa*. Additionally, it has been observed that several phytochemicals, which are often used in traditional medicine and cooking, have demonstrated the ability to fight against different clinically relevant pathogens, including *P. aeruginosa*. In this sense, we sought to determine the in silico interaction ability of various phytochemicals on proteins associated with EPS biosynthesis in *P. aeruginosa* by applying predictive docking and coarse-grained molecular dynamics analyses (elastic network models) to study changes at the level of intrinsic structural flexibility of the considered protein targets after binding. All the phytochemical compounds studied showed thermodynamically favorable bonds and stable unions with all the proteins studied over time. Epigallocatechin and curcumin were the phytochemicals with the most favorable and stable relative binding energies in all cases. These results correspond to the compounds in clinical trials against clinically relevant pathogens. Therefore, more studies are needed to continue understanding the mechanism of action of these promising compounds against such important pathogens at a global public health level.

Keywords: elastic network models; curcumin; epigallocatechin; biofilms.

© 2024 by the authors. This article is an open-access article distributed under the terms and conditions of the Creative Commons Attribution (CC BY) license (<https://creativecommons.org/licenses/by/4.0/>).

1. Introduction

Pseudomonas aeruginosa is an opportunistic pathogen of clinical interest, which can become resistant to multiple antibiotics and possesses various virulence factors, such as the production of mucopolysaccharide [1,2]. The production of mucopolysaccharide by *P. aeruginosa* in hospital infections is a topic of great interest because it represents a problem as

it is a mechanism that gives this bacterium greater resistance to drugs and can also complicate the respiratory pathways of patients in intensive care [2-4]. Various genetic determinants have been described that encode diverse proteins associated with the biosynthesis of mucopolysaccharide in *P. aeruginosa*, among which the “Las” systems stand out, which are part of the regulation of a complex mechanism known as “Quorum Sensing” in *P. aeruginosa* [5-9].

Quorum sensing (QS) is a process in which cells regulate the expression of their genes based on cell population density. This is achieved by releasing molecules called autoinducers, which can act on the cell that released them and trigger a response throughout the population. This process is a form of cellular communication between cells of the same organism or between different individuals [5,10]. The las system is one of the complete quorum-sensing systems present in the opportunistic human pathogen *P. aeruginosa*. This type of system is known to control the expression of various virulence genes in response to bacterial cell density. The las system contains homologs of the prototypic lux quorum-sensing system from *Vibrio fischeri*. It consists of the transcriptional activator protein LasR and LasI, which directs the synthesis of the autoinducer PAI-1 [N-(3-oxododecanoyl)-L-homoserine lactone]. This system has been shown to activate the expression of determinants such as lasI, lasB, and lasA [8,9,11-14].

On the other hand, it has been noted that various phytochemical compounds commonly used in both traditional medicine and culinary, such as curcumin [15-18], piperine [19-21], green tea or epigallocatechin gallate (EGCG) [22-24], among others [25,26], have shown antimicrobial activity against various pathogens of clinical interest including *P. aeruginosa* [19,27,28]. Some efforts have been made previously to study the interaction of various phytochemicals with *P. aeruginosa* proteins [29-31]; however, more studies are needed on the binding ability of popular natural compounds on proteins associated with mucopolysaccharide biosynthesis [32,33].

The aforementioned is important because it is known that changes in the intrinsic stiffness or flexibility of a protein due to the effect of an external agent, such as a drug, can be decisive in altering the biological activity of a said protein, which could represent a potential inhibitory effect of interest at the biomedical level [34-36]. In this sense, we sought to determine the in silico interaction ability of various phytochemicals on proteins associated with mucopolysaccharide biosynthesis in *P. aeruginosa* by applying predictive docking and coarse-grained molecular dynamics analyses (elastic network models) to study changes at the level of intrinsic structural flexibility of the considered protein targets after binding.

2. Materials and Methods

2.1. Selection and preparation of protein structures from databases.

Protein crystallographic structures related to the mucoid phenotype in *P. aeruginosa* were selected. The structures selected were LasR (PDB: 3IX3), LasI (PDB: 1RO5), LasB (PDB: 6FZX), and LasA (PDB: 3IT5). These structures were obtained from the RCSB-protein data bank in PDB format (<https://www.rcsb.org/>). The Molegro Molecular package was utilized for viewing and preparing the files.

2.2. Selection and preparation of phytochemicals from databases.

After conducting a literature review, we examined eighteen phytochemicals with known antiviral properties, including Allicin [37], Capsaicin [38], Carvacrol [39], Cinnamic acid [40], Curcumin [41], Eucalyptol [42], Gallic acid [43], Piperine [44], Quercetin [45,46,47], and Epigallocatechin [48]. The 3D structures of these drugs were obtained from the PubChem database (<https://pubchem.ncbi.nlm.nih.gov/>) in SDF format [49] and converted to PDB format using the Online SMILES Translator (<https://cactus.nci.nih.gov/translate/>).

2.3. Molecular docking and redocking.

We used CB-DOCK2 (<https://cadd.labshare.cn/cb-dock2/>) [50,51] to perform molecular docking analysis to determine the binding of phytochemical compounds to LasR (PDB: 3IX3), LasI, LasB, and LasA. The most favorable position of each predicted complex by CB-DOCK2 was analyzed using Molegro Molecular Viewer (MMV) by calculating the MolDock Score and Plants Score functions [52]. In addition to using the CB-DOCK2 scoring function, we also conducted a comparative analysis using other scoring functions included in the MMV package. Specifically, we considered the MolDock Score, a new hybrid heuristic search algorithm that combines differential evolution with a cavity prediction algorithm and uses an extension of the Piecewise Linear Potential (PLP) as its scoring function. This extension takes into account directionality, hydrogen bond charges, and electrostatic interactions. It has proven to be one of the most accurate for rapid screenings because the best-ranked poses are re-ranked using a more complex scoring function that adds an sp²-sp² torsion term to the hydrogen bond calculation and a Lennard-Jones potential term to the score [53]. In parallel, to obtain an approximate evaluation of the best-ranked poses, we also used a binding affinity estimation, so we also considered the Plants Score (Protein-Ligand ANT System) algorithm, which is based on a stochastic optimization algorithm called ant colony optimization (ACO) and whose empirical scoring function is similarly based on a PLP similar to that used by MolDock but integrates more interaction types (repulsive, attractive, non-polar, hydrogen bonds, and metallic), making it more conservative than MolDock and recommended as a subsequent re-ranking strategy [53,54].

2.4. Molecular dynamics of ligand-protein complexes.

The PDB files of the target proteins, which were static and lacked H-atoms, were modified and optimized to better understand their dynamic and functional behavior after being conjugated with ligands. We used the UNRES online server [55-60] to perform molecular dynamics (MD) simulations of the best protein-ligand interactions and analyze the dynamic stability of the protein systems when docked with the best ligands. This recently developed server uses physics-based coarse-grain simulations to predict protein dynamics and thermodynamics. It can accurately predict protein structure, dynamics, and interactions over longer periods [55-60]. The MD method based on coarse-grain was carried out at 300K using the Berendsen thermostat for conformational search. Each MD trajectory had an integration time of 48.9fs, and other parameters were set to default values for better system simulation. We performed MD runs to predict root mean square deviation (RMSD), potential energy, radius of gyration (Rg), and root mean square fluctuation (RMSF). The final simulation time was 100ns, and output files were retrieved from the UNRES server and visualized using MMV software.

3. Results and Discussion

All the phytochemical compounds studied showed thermodynamically favorable bonds against all the proteins considered in this study (Table 1). The overall thermodynamic mean for all the predicted interactions for the proteins was -51.06 ± 13.39 kcal/mol, with less favorable minimum values for Eucalyptol and maximum or more favorable for curcumin of -30.17 kcal/mol and -69.98 kcal/mol, respectively. Specifically, for the LasA protein, the thermodynamic mean was -48.50 ± 12.37 kcal/mol, also with less favorable values for Eucalyptol (-26.08 kcal/mol) and more favorable for curcumin (-65.52 kcal/mol). For the LasB system, the predicted thermodynamic mean was -52.89 ± 16.63 kcal/mol, with less favorable values for Eucalyptol (-21.86 kcal/mol) and more favorable for Epigallocatechin (-73.35 kcal/mol). For LasI, the trend was similar to that predicted against LasB, with a thermodynamic mean of -43.09 ± 9.90 kcal/mol, with less favorable values for Eucalyptol (-27.28 kcal/mol), and more favorable for Epigallocatechin (-60.31 kcal/mol). While for the LasR system, the predicted thermodynamic mean was -59.76 ± 16.93 kcal/mol, with less favorable values for Allicin (-38.73 kcal/mol) and more favorable for curcumin (-85.71 kcal/mol). These results show that Epigallocatechin and Curcumin were the phytochemical compounds with the most thermodynamically favorable relative binding energies in all cases, with Eucalyptol being the compound with the least number of favorable interactions.

Table 1. Phytochemical compounds and relative binding energy correspond to the scoring functions considered.

Phytochemical*	Kcal/mol											
	CB-Dock2/Vina Score				MolDock Score				PLANT Score			
	LasA	LasB	LasI	LasR	LasA	LasB	LasI	LasR	LasA	LasB	LasI	LasR
Epigallocatechin	-8.5	-8.3	-7.0	-9.0	-123.4	-145.6	-132.0	-173.2	-60.1	-66.1	-42.0	-60.0
Quercetin	-7.9	-8.2	-6.9	-10.3	-104.5	-124.2	-89.6	-116.7	-68.6	-71.2	-61.7	-69.2
Curcumin	-7.5	-8.1	-6.3	-10.1	-127.2	-116.8	-90.3	-155.9	-61.9	-66.6	-53.7	-91.2
Piperine	-7.5	-8.2	-6.7	-10.9	-79.3	-114.7	-75.0	-119.6	-52.4	-76.4	-55.3	-83.0
Capsaicin	-6.8	-7.7	-6.3	-9.6	-91.1	-122.1	-84.3	-122.6	-43.1	-64.8	-50.4	-77.9
Cinnamic acid	-6.5	-6.4	-5.9	-7.0	-66.0	-67.1	-60.6	-71.7	-63.9	-59.6	-54.1	-61.1
Carvacrol	-6.1	-6.2	-5.6	-7.3	-60.6	-58.3	-52.7	-74.3	-64.6	-62.4	-54.0	-64.4
Gallic acid	-6.0	-5.5	-5.2	-6.8	-83.0	-72.2	-54.8	-87.2	-62.6	-56.9	-48.3	-56.1
Eucalyptol	-4.8	-4.3	-5.0	-6.7	-27.6	-18.7	-31.7	-54.5	-45.8	-42.6	-45.1	-60.4
Allicin	-4.1	-4.1	-4.6	-5.1	-53.1	-59.5	-46.7	-55.4	-50.3	-54.0	-50.8	-55.7

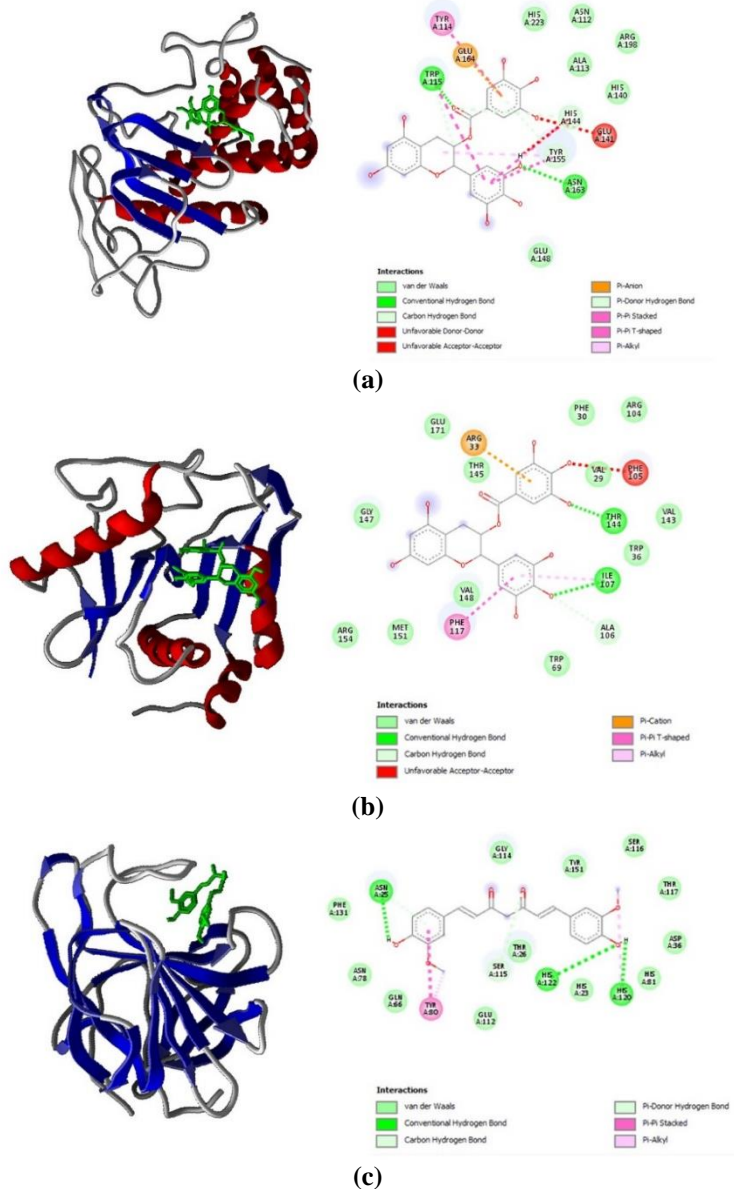
*, The structures of these drugs were obtained from the PubChem database (<https://pubchem.ncbi.nlm.nih.gov/>) in SDF format [49].

When studying the three most favorable poses or the first three places predicted for each compound, it was observed that Epigallocatechin was the phytochemical that presented the most favorable predictions for all the proteins studied, represented by 50% of favorable complexes both in the poses located in the first place of the rankings and in the poses predicted in second place, also gathering 50% of favorable complexes (Table 2). Followed by curcumin, with $\approx 66\%$ of favorable complexes in the first poses and the rest only from the poses predicted in third place (Table 2). Quercetin gathered $\approx 66\%$ of its most favorable complexes in poses located in second place and the rest in third place (Table 2). Finally, Piperine was the last compound to enter within the first three predicted favorable poses, but it concentrated 100% of its complexes in the third place of the poses (Table 2).

Table 2. Ranking of the most favorable ligand interactions.

Ranking	# of most favorable poses/protein system with favorable interaction			
	Epigallocatechin	Curcumin	Quercetin	Piperine
1°	2 / LasB and LasI	2 / LasA and LasR	-	-
2°	2 / LasR and LasA	-	2 / LasB and LasI	-
3°	-	1 / LasI	1 / LasA	2 / LasB and LasR

All predicted interactions for protein complexes with Epigallocatechin and Curcumin had a minimum of minus 2 hydrogen bonds and more than 6 van der Waals interactions. The highest number of hydrogen bonds and van der Waals interactions were predicted for complexes with curcumin (see Figure 1). Specifically, the Epigallocatechin + LasB complex had 15% (2/13) hydrogen bond interactions, followed by 46% (6/13) van der Waals interactions (see Figure 1A). The nature of most of the interactions of the Epigallocatechin + LasI complex were 11% (2/18) hydrogen bonds and 66% (12/18) van der Waals interactions (see Figure 1B). On the other hand, for the Curcumin + LasA complex, 17% (3/17) hydrogen bonds were predicted, and 70% (12/17) van der Waals interactions (see Figure 1C), while most of the interactions of the curcumin + LasR complex were 12% (3/25) hydrogen bonds and 48% (12/25) van der Waals interactions (see Figure 1D).



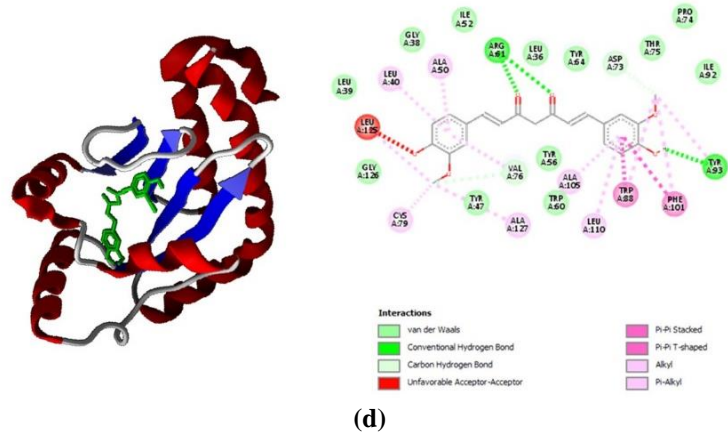


Figure 1. 2D diagram and secondary structures of the most favorable molecular docking of **a)** Epigallocatechin + LasB; **b)** Epigallocatechin + LasI; **c)** Curcumin + LasA; **d)** Curcumin + LasR.

Since the phytochemicals Epigallocatechin and Curcumin were the compounds that showed the most favorable couplings, each with a different pair of proteins, the stability of the Curcumin + LasA and Curcumin + LasR complexes (see Figure 2) were studied, as well as the Epigallocatechin + LasB and Epigallocatechin + LasI complexes (see Figure 3) as a function of time after molecular dynamics at 100ns of simulation.

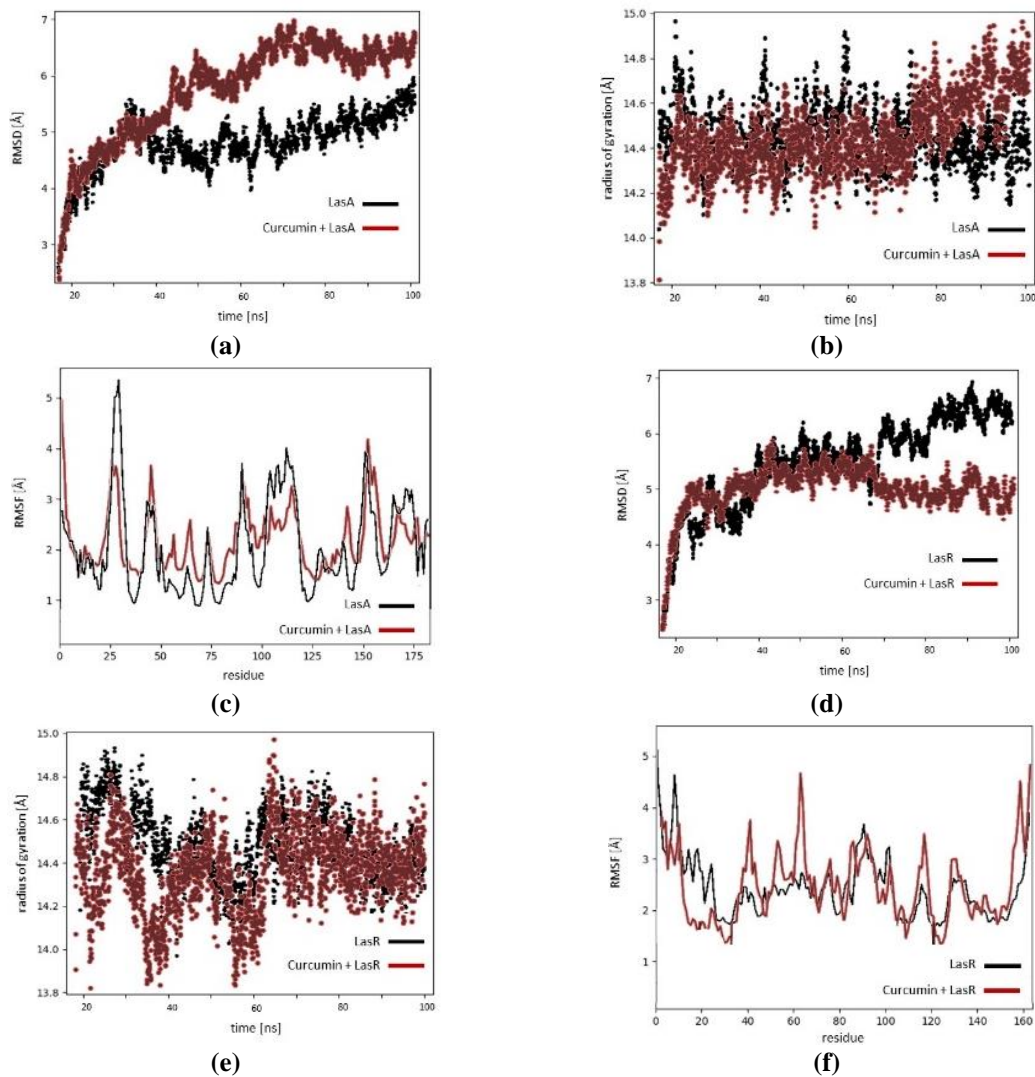


Figure 2. RMSD, Rg and RMSF of LasA (**a, b, c**), LasR (**d, e, f**) in the presence and absence of curcumin, respectively.

After the simulations, it was observed that all the complexes studied were stable as a function of the simulation time considered at the level of conformational fluctuations (RMSD, Rg, and RMSF) and energetic (potential energy of the system). Specifically, an $\text{RMSD} \leq 6\text{\AA}$ was predicted for all complexes, with a difference of only $\approx 0.5\text{\AA}$ between protein systems in the presence and absence of ligands. Regarding Rg, all protein systems were predicted to be stable with few fluctuations in trajectories in the presence and absence of ligands, just as predicted for RMSD, with a difference in minimum energy structures obtained between $0.1 - 0.5\text{\AA}$. The stability of the complexes as a function of simulation time was validated at the level of local fluctuations of each one in terms of RMSF, showing an average for all systems in the presence and absence of ligands $\leq 3\text{\AA}$. On the other hand, concerning the potential energy of protein systems in the presence and absence of ligands after MD simulation, it was predicted that all systems are thermodynamically favorable throughout the time considered in this study (Figure 4). Specifically, protein systems that interacted with curcumin had an average potential energy of $\approx -560\text{kcal/mol}$, with slightly more favorable systems in the presence of ligands.

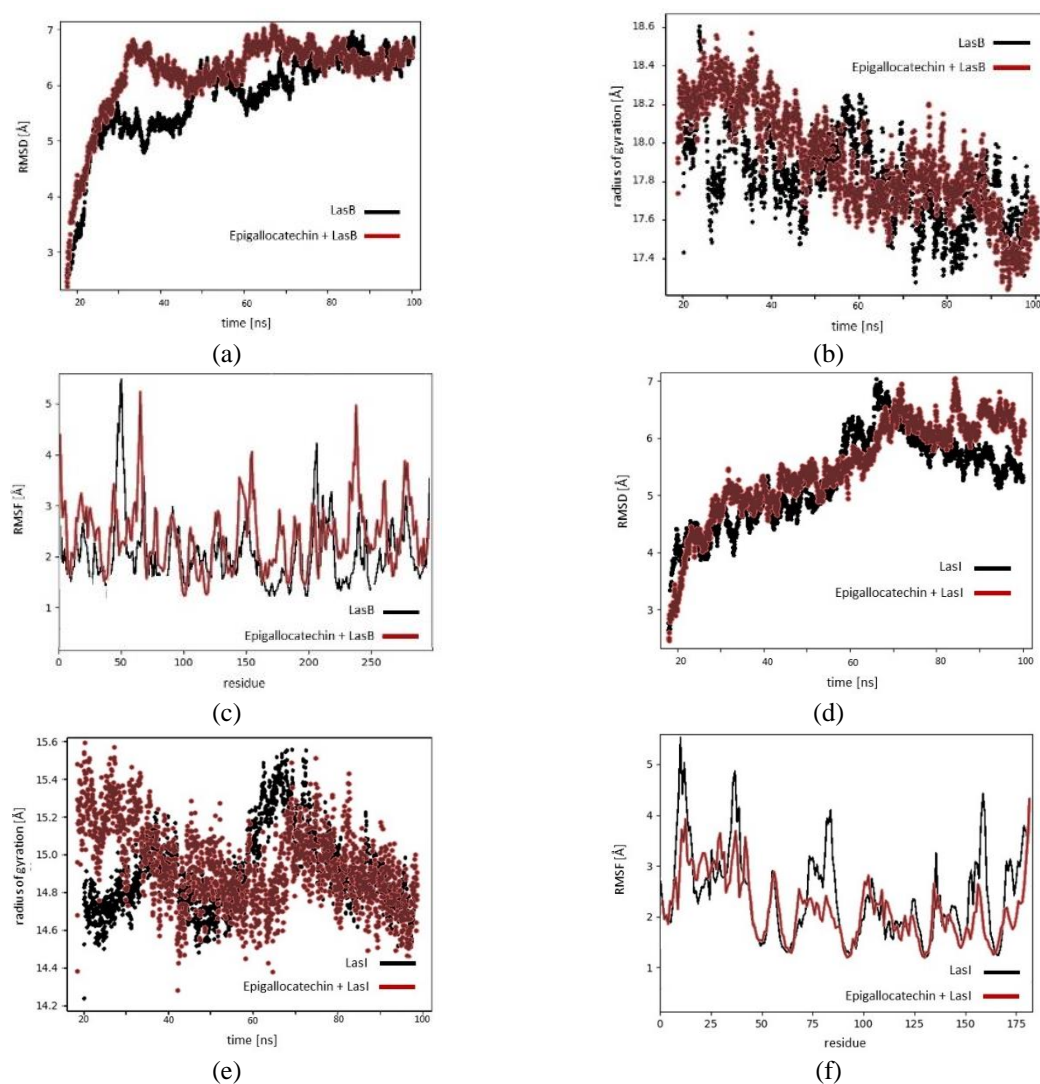


Figure 3. RMSD, Rg and RMSF of LasB (a, b, c); LasI (d, e, f) in the presence and absence of Epigallocatechin, respectively.

While with Epigallocatechin's thermodynamic average at the end of MD simulation was $\approx -770\text{kcal/mol}$ for all systems. The Curcumin + LasA complex was the one that presented the greatest difference at potential energy level after 100ns of simulation, with a decrease in system

energy in the presence of ligand by ≈ -50 kcal/mol, indicative of a thermodynamically more favorable system compared to free protein.

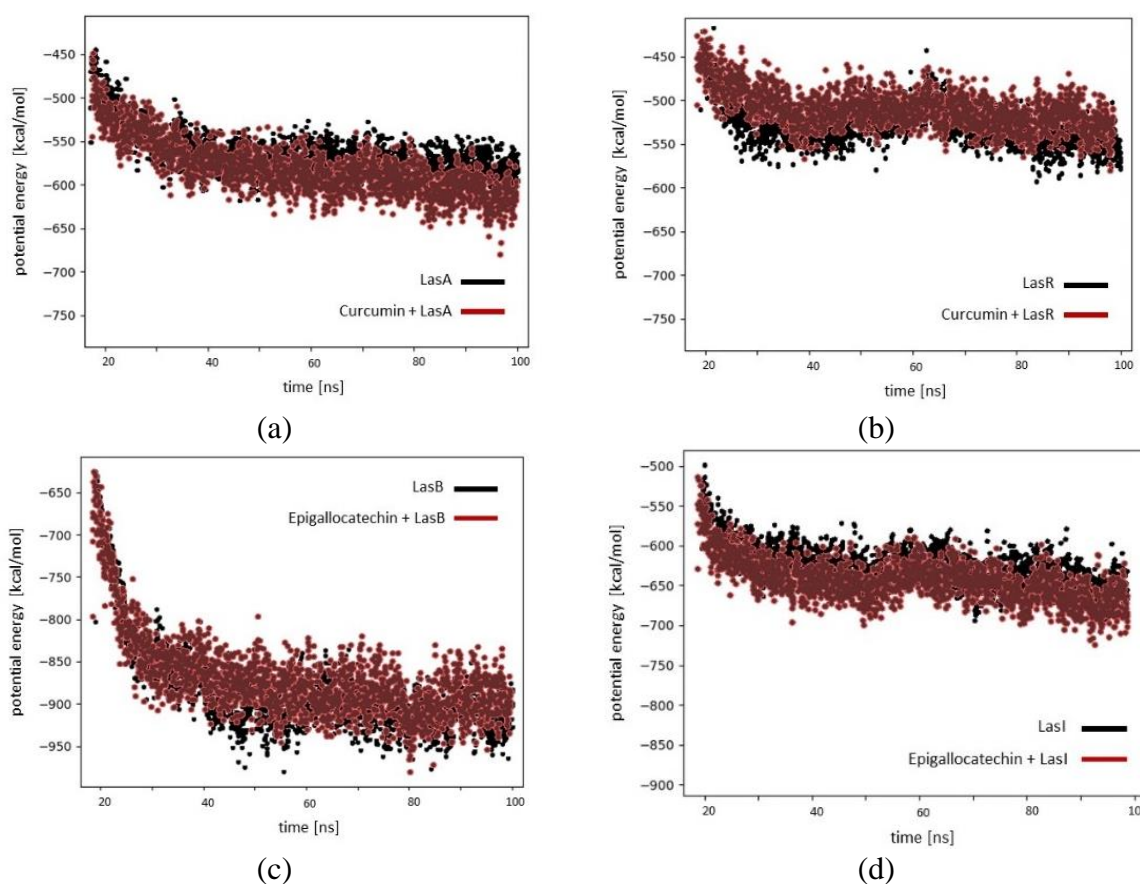


Figure 4. The potential energy of (a) LasA; (b) LasR in the presence and absence of curcumin, respectively; and of (c) LasB; (d) LasI in the presence and absence of Epigallocatechin, respectively.

The results obtained in this study are consistent with other molecular docking studies that have found that the phytochemicals Epigallocatechin and Curcumin tend to have very favorable relative binding energies, as well as stable MD bonds against clinically relevant pathogens related to *P. aeruginosa* [61], and pandemic-causing pathogens [62]. In addition, the interaction of these types of compounds with the potential inhibitory activity of proteins of interest associated with pathogens such as *P. aeruginosa* has already been studied [63]. The fact that Epigallocatechin and Curcumin were the phytochemical compounds with the most thermodynamically favorable relative binding energies in all cases is not a coincidence. It corresponds to including these compounds in clinical trials against unrelated clinically relevant pathogens [64]. Our observations hold great importance due to the increasing prevalence of multi-drug resistant bacteria, which has made it necessary to develop new strategies for studying potential microbial targets and thus contribute to the fight against bacterial invasion and colonization. Quorum sensing (QS) is a communication system used by bacteria such as *P. aeruginosa* that involves signaling molecules to control virulence, bioluminescence, and survival. QS also plays a role in biofilm formation, protecting conventional antimicrobial compounds. Biofilms create specific environments that allow bacteria to tolerate antibiotics. This is why seeking QS inhibition through alternative compounds can improve the effectiveness of traditional antibiotics, prevent the spread of resistant strains, and reduce biofilm formation [63]. However, the search for effective phytochemicals against pathogens continues, and safety concerns loom over the application of phytomedicines, especially due to the scarcity of available data on the safety, efficacy, and quality of most of these plants.

Uninvestigated use of purified compounds is not recommended, and these phytochemicals must first undergo adequate safety and efficacy testing, although it has been noted that phytochemicals are inherently safe to use because of their biocompatibility, ecology and lower toxicity compared to xenobiotics [63].

4. Conclusions

All the phytochemical compounds studied showed thermodynamically favorable bonds and stability over time in dynamic terms (at the level of distance and residue fluctuation) against all the proteins studied. Epigallocatechin and curcumin were the phytochemicals with the most thermodynamically favorable and stable relative binding energies in all cases, with Eucalyptol being the least favorable compound. In this sense, the fact that Epigallocatechin and Curcumin were the phytochemical compounds with the most thermodynamically favorable relative binding energies in all cases corresponds to including these compounds in clinical trials against unrelated clinically relevant pathogens. Therefore, more studies are necessary to continue understanding the mechanism of action of these promising compounds against such important pathogens at a global public health level.

Funding

This research received no specific grant from public, commercial, or not-for-profit funding agencies.

Acknowledgments

This research has no acknowledgment.

Conflicts of Interest

The authors declare that they have no known competing financial interests or personal relationships that could have appeared to influence the work reported in this paper.

References

1. Depond, M.; Henry, B.; Buffet, P.; Ndour, P.A. Methods to Investigate the Deformability of RBC During Malaria. *Front. Physiol.* **2020**, *10*, 1613, <https://doi.org/10.3389/fphys.2019.01613>.
2. Meldrum, O.W.; Chotirmall, S.H. Mucus, Microbiomes and Pulmonary Disease. *Biomedicines* **2021**, *9*, 675, <https://doi.org/10.3390/biomedicines9060675>.
3. Myszor, I.T.; Gudmundsson, G.H. Modulation of innate immunity in airway epithelium for host-directed therapy. *Front. Immunol.* **2023**, *14*, 1197908, <https://doi.org/10.3389/fimmu.2023.1197908>.
4. He, S.; Gui, J.; Xiong, K.; Chen, M.; Gao, H.; Fu, Y. A roadmap to pulmonary delivery strategies for the treatment of infectious lung diseases. *J. Nanobiotechnol.* **2022**, *20*, 101, <https://doi.org/10.1186/s12951-022-01307-x>.
5. Hall-Stoodley, L.; McCoy, K.S. Biofilm aggregates and the host airway-microbial interface. *Front. Cell. Infect. Microbiol.* **2022**, *12*, 969326, <https://doi.org/10.3389/fcimb.2022.969326>.
6. Chadha, J.; Harjai, K.; Chhibber, S. Revisiting the virulence hallmarks of *Pseudomonas aeruginosa*: a chronicle through the perspective of quorum sensing. *Environ. Microbiol.* **2022**, *24*, 2630-2656, <https://doi.org/10.1111/1462-2920.15784>.
7. Li, Q.; Mao, S.; Wang, H.; Ye, X. The Molecular Architecture of *Pseudomonas aeruginosa* Quorum-Sensing Inhibitors. *Mar. Drugs* **2022**, *20*, 488, <https://doi.org/10.3390/md20080488>.

8. Chadha, J.; Harjai, K.; Chhibber, S. Repurposing phytochemicals as anti-virulent agents to attenuate quorum sensing-regulated virulence factors and biofilm formation in *Pseudomonas aeruginosa*. *Microb. Biotechnol.* **2022**, *15*, 1695-1718, <https://doi.org/10.1111/1751-7915.13981>.
9. Soto-Aceves, M.P.; Cocotl-Yañez, M.; Servín-González, L.; Soberón-Chávez, G. The Rhl Quorum-Sensing System Is at the Top of the Regulatory Hierarchy under Phosphate-Limiting Conditions in *Pseudomonas aeruginosa* PAO1. *J. Bacteriol.* **2021**, *203*, 10-1128, <https://doi.org/10.1128/jb.00475-20>.
10. İnat, G.; Sırıken, B.; Başkan, C.; Erol, İ.; Yıldırım, T.; Çiftçi, A. Quorum sensing systems and related virulence factors in *Pseudomonas aeruginosa* isolated from chicken meat and ground beef. *Sci. Rep.* **2021**, *11*, 15639, <https://doi.org/10.1038/s41598-021-94906-x>.
11. Ge, C.; Yu, Z.; Sheng, H.; Shen, X.; Sun, X.; Zhang, Y.; Yan, Y.; Wang, J.; Yuan, Q. Redesigning regulatory components of quorum-sensing system for diverse metabolic control. *Nat. Commun.* **2022**, *13*, 2182, <https://doi.org/10.1038/s41467-022-29933-x>.
12. Hendiani, S.; Pornour, M.; Kashef, N. Sub-lethal antimicrobial photodynamic inactivation: an in vitro study on quorum sensing-controlled gene expression of *Pseudomonas aeruginosa* biofilm formation. *Lasers Med. Sci.* **2019**, *34*, 1159-1165, <https://doi.org/10.1007/s10103-018-02707-y>.
13. Vijayakumar, K.; Ramanathan, T. *Musa acuminata* and its bioactive metabolite 5-Hydroxymethylfurfural mitigates quorum sensing (*las* and *rhl*) mediated biofilm and virulence production of nosocomial pathogen *Pseudomonas aeruginosa* in vitro. *J. Ethnopharmacol.* **2020**, *246*, 112242, <https://doi.org/10.1016/j.jep.2019.112242>.
14. Zhang, Y.; He, X.; Cheng, P.; Li, X.; Wang, S.; Xiong, J.; Li, H.; Wang, Z.; Yi, H.; Du, H.; Liu, J.; Chen, H. Effects of a novel anti-biofilm peptide CRAMP combined with antibiotics on the formation of *Pseudomonas aeruginosa* biofilms. *Microb. Pathog.* **2021**, *152*, 104660, <https://doi.org/10.1016/j.micpath.2020.104660>.
15. Pesci, E.C.; Pearson, J.P.; Seed, P.C.; Iglewski, B.H. Regulation of *las* and *rhl* quorum sensing in *Pseudomonas aeruginosa*. *J. Bacteriol.* **1997**, *179*, 3127-3132, <https://doi.org/10.1128/jb.179.10.3127-3132.1997>.
16. Omorodion, N.J.; Ujoh, E.C. Antimicrobial activities of aqueous and ethanolic extracts of some natural spices (garlic, turmeric, thyme and onions) on some clinical isolates. *GSC Biol. Pharm. Sci.* **2022**, *19*, 335-345, <https://doi.org/10.30574/gscbps.2022.19.1.0094>.
17. Isopencu, G.; Deleanu, I.; Busuioc, C.; Oprea, O.; Surdu, V.A.; Bacalum, M.; Stoica, R.; Stoica-Guzun, A. Bacterial Cellulose—Carboxymethylcellulose Composite Loaded with Turmeric Extract for Antimicrobial Wound Dressing Applications. *Int. J. Mol. Sci.* **2023**, *24*, 1719, <https://doi.org/10.3390/ijms24021719>.
18. Basak, P.; Adhikary, T.; Das, P.; Biswas, S. Phytochemical analysis and comparative study of antibacterial effect of turmeric extracts using different solvent. *IOP Conf. Ser.: Mater. Sci. Eng.* **2018**, *410*, 012018, <https://doi.org/10.1088/1757-899X/410/1/012018>.
19. Khan, M.A.; Moghul, N.B.; Butt, M.A.; Kiyani, M.M.; Zafar, I.; Bukhari, A.I. Assessment of antibacterial and antifungal potential of *Curcuma longa* and synthesized nanoparticles: A comparative study. *J. Basic Microbiol.* **2021**, *61*, 603-611, <https://doi.org/10.1002/jobm.202100010>.
20. Alves, F.S.; Cruz, J.N.; de Farias Ramos, I.N.; do Nascimento Brandão, D.L.; Queiroz, R.N.; da Silva, G.V.; da Silva, G.V.; Dolabela, M.F.; da Costa, M.L.; Khayat, A.S.; do Rego, J.d.A.R.; Brasil, D.d.S.B. Evaluation of Antimicrobial Activity and Cytotoxicity Effects of Extracts of *Piper nigrum* L. and Piperine. *Separations* **2023**, *10*, 21, <https://doi.org/10.3390/separations10010021>.
21. Manjunath, G.B.; Awasthi, S.P.; Zahid, M.S.H.; Hatanaka, N.; Hinenoya, A.; Iwaoka, E.; Aoki, S.; Ramamurthy, T.; Yamasaki, S. Piperine, an active ingredient of white pepper, suppresses the growth of multidrug-resistant toxigenic *Vibrio cholerae* and other pathogenic bacteria. *Lett. Appl. Microbiol.* **2022**, *74*, 472-481, <https://doi.org/10.1111/lam.13646>.
22. Habib, T.; Parvin, F. Effects of Natural compound “Piperine” on the growth and Adhesive Properties of Streptococcus Mutans Bacterial Biofilm. *J. Bangladesh Coll. Phys. Surg.* **2023**, *41*, 33-39, <https://doi.org/10.3329/jbcps.v41i1.63257>.
23. Widadalla, H.A.; Yassin, L.F.; Alrasheid, A.A.; Ahmed, S.A.R.; Widdatallah, M.O.; Eltilib, S.H.; Mohamed, A.A. Green synthesis of silver nanoparticles using green tea leaf extract, characterization and evaluation of antimicrobial activity. *Nanoscale Adv.* **2022**, *4*, 911-915, <https://doi.org/10.1039/D1NA00509J>.
24. Siriphap, A.; Kiddee, A.; Duangjai, A.; Yosboonruang, A.; Pook-In, G.; Saokaew, S.; Suthengkul, O.; Rawangkan, A. Antimicrobial Activity of the Green Tea Polyphenol (–)–Epigallocatechin-3-Gallate (EGCG) against Clinical Isolates of Multidrug-Resistant *Vibrio cholerae*. *Antibiotics* **2022**, *11*, 518, <https://doi.org/10.3390/antibiotics11040518>.

25. Sarkar, A.; Alam, M.; Roy, P.; Biswas, R.; Haque, M.I. Physicochemical, antioxidant and antimicrobial activities of green teas manufactured from common tea clones of different gardens in Bangladesh. *J. Agric. Food Res.* **2022**, *10*, 100407, <https://doi.org/10.1016/j.jafr.2022.100407>.
26. Jadimurthy, R.; Jagadish, S.; Nayak, S.C.; Kumar, S.; Mohan, C.D.; Rangappa, K.S. Phytochemicals as Invaluable Sources of Potent Antimicrobial Agents to Combat Antibiotic Resistance. *Life* **2023**, *13*, 948, <https://doi.org/10.3390/life13040948>.
27. Zeroual, A.; Sakar, E.H.; Mahjoubi, F.; Chaouch, M.; Chaqroune, A.; Taleb, M. Effects of Extraction Technique and Solvent on Phytochemicals, Antioxidant, and Antimicrobial Activities of Cultivated and Wild Rosemary (*Rosmarinus officinalis* L.) from Taounate Region (Northern Morocco). *Biointerface Res. Appl. Chem.* **2022**, *12*, 8441-8452, <https://doi.org/10.33263/BRIAC126.84418452>.
28. Jayathilake, A.L.; Jayasinghe, M.A.; Walpita, J. Development of ginger, turmeric oleoresins and pomegranate peel extracts incorporated pasteurized milk with pharmacologically important active compounds. *Appl. Food Res.* **2022**, *2*, 100063, <https://doi.org/10.1016/j.afres.2022.100063>.
29. Saod, W.M.; Hamid, L.L.; Alaallah, N.J.; Ramizy, A. Biosynthesis and antibacterial activity of manganese oxide nanoparticles prepared by green tea extract. *Biotechnol. Rep.* **2022**, *34*, e00729, <https://doi.org/10.1016/j.btre.2022.e00729>.
30. Baburam, S.; Ramasamy, S.; Shanmugam, G.; Mathanmohun, M. Quorum Sensing Inhibitory Potential and Molecular Docking Studies of *Phyllanthus emblica* Phytochemicals Against *Pseudomonas aeruginosa*. *Appl. Biochem. Biotechnol.* **2022**, *194*, 434-444, <https://doi.org/10.1007/s12010-021-03683-w>.
31. Shastry, R.P.; Abhinand, C.S. Targeting the *Pseudomonas aeruginosa* quorum sensing system to inhibit virulence factors and eradicate biofilm formation using AHL-analogue phytochemicals. *J. Biomol. Struct. Dyn.* **2023**, 1-10, <https://doi.org/10.1080/07391102.2023.2202270>.
32. Degfie, T.; Endale, M.; Tafese, T.; Dekebo, A.; Shenkute, K. In vitro antibacterial, antioxidant activities, molecular docking, and ADMET analysis of phytochemicals from roots of *Hydnora johannis*. *Appl. Biol. Chem.* **2022**, *65*, 76, <https://doi.org/10.1186/s13765-022-00740-8>.
33. Nath, H.; Khataniar, A.; Bania, K.K.; Mukerjee, N.; Al-Hussain, S.A.; Zaki, M.E.A.; Rajkhowa, S. Nano-functionalization and evaluation of antimicrobial activity of *Tinospora cordifolia* against the TolB protein of *Pseudomonas aeruginosa*—An antibacterial and computational study. *Front. Microbiol.* **2023**, *14*, 1138106, <https://doi.org/10.3389/fmicb.2023.1138106>.
34. Anju, V.T.; Busi, S.; Mohan, M.S.; Ranganathan, S.; Ampasala, D.R.; Kumavath, R.; Dyavaiah, M. *In vivo*, *in vitro* and molecular docking studies reveal the anti-virulence property of hispidulin against *Pseudomonas aeruginosa* through the modulation of quorum sensing. *Int. Biodeterior. Biodegrad.* **2022**, *174*, 105487, <https://doi.org/10.1016/j.ibiod.2022.105487>.
35. Calvo-Alvarez, E.; Dolci, M.; Perego, F.; Signorini, L.; Parapini, S.; D'Alessandro, S.; Denti, L.; Basilico, N.; Taramelli, D.; Ferrante, P.; Delbue, S. Antiparasitic Drugs against SARS-CoV-2: A Comprehensive Literature Survey. *Microorganisms* **2022**, *10*, 1284, <https://doi.org/10.3390/microorganisms10071284>.
36. Dayananda, A.; Dennison, T.S.H.; Fonseka, H.Y.Y.; Avestan, M.S.; Wang, Q.; Tehver, R.; Stan, G. Allosteric communication in the gating mechanism for controlled protein degradation by the bacterial ClpP peptidase. *J. Chem. Phys.* **2023**, *158*, 125101, <https://doi.org/10.1063/5.0139184>.
37. Joshi, B.P.; Bhandare, V.V.; Vankawala, M.; Patel, P.; Patel, R.; Vyas, B.; Krishnamurty, R. Friedelin, a novel inhibitor of CYP17A1 in prostate cancer from *Cassia tora*. *J. Biomol. Struct. Dyn.* **2022**, *41*, 9695-9720, <https://doi.org/10.1080/07391102.2022.2145497>.
38. Xie, Y.; Chen, Y.; Guo, Y.; Huang, Y.; Zhu, B. Allicin and Glycyrrhizic Acid Display Antiviral Activity Against Latent and Lytic Kaposi Sarcoma-associated Herpesvirus. *Infect. Microbes Dis.* **2020**, *2*, 30-34, <https://doi.org/10.1097/IM9.000000000000016>.
39. Tang, K.; Zhang, X.; Guo, Y. Identification of the dietary supplement capsaicin as an inhibitor of Lassa virus entry. *Acta Pharm. Sin. B* **2020**, *10*, 789-798, <https://doi.org/10.1016/j.apsb.2020.02.014>.
40. Bansal, A.; Jan, I.; Sharma, N.R. Anti-phytoviral Activity of Carvacrol vis-a-vis Cauliflower Mosaic Virus (CaMV). *Proc. Natl. Acad. Sci. India, Sect. B: Biol. Sci.* **2020**, *90*, 981-988, <https://doi.org/10.1007/s40011-020-01166-2>.
41. Silva, A.T.; Bento, C.M.; Pena, A.C.; Figueiredo, L.M.; Prudêncio, C.; Aguiar, L.; Silva, T.; Ferraz, R.; Gomes, M.S.; Teixeira, C.; Gomes, P. Cinnamic Acid Conjugates in the Rescuing and Repurposing of Classical Antimalarial Drugs. *Molecules* **2020**, *25*, 66, <https://doi.org/10.3390/molecules25010066>.
42. Do Bonfim, C.M.; Monteleoni, L.F.; Calmon, M.d.F.; Cândido, N.M.; Provazzi, P.J.S.; Lino, V.d.S.; Rabachini, T.; Sichero, L.; Villa, L.L.; Quintana, S.M.; dos Santos Melli, P.P.; Primo, F.L.; Amantino, C.F.;

- Tedesco, A.C.; Boccardo, E.; Rahal, P. Antiviral activity of curcumin-nanoemulsion associated with photodynamic therapy in vulvar cell lines transducing different variants of HPV-16. *Artif. Cells Nanomed. Biotechnol.* **2020**, *48*, 515-524, <https://doi.org/10.1080/21691401.2020.1725023>.
43. Patra, J.K.; Das, G.; Bose, S.; Banerjee, S.; Vishnuprasad, C.N.; del Pilar Rodriguez, M.; Shin, H.-S. Star anise (*Illicium verum*): Chemical compounds, antiviral properties, and clinical relevance. *Phytother. Res.* **2020**, *34*, 1248-1267, <https://doi.org/10.1002/ptr.6614>.
 44. Arsianti, A.; Bahtiar, A.; Fadilah, F.; Wangsaputra, V.K.; Paramita, R.I.; Azizah, N.N.; Nadapdap, L.D.; Fajrin, A.M.; Tanimoto, H.; Kakiuchi, K. Synthesis, Characterization, and Cytotoxicity Evaluation of Gallic Acid Nanoparticles Towards Breast T47D Cancer Cells *Pharmacognosy J.* **2020**, *12*, 321-327, <http://doi.org/10.5530/pj.2020.12.51>.
 45. Chandani, S.R.; Thorat, P.A.; Nanda, R.K.; Chitlange, S.S. Docking of Phytoconstituents of *Cynodon dactylon* on NS2B NS3 protease domain of Dengue virus. *Res. J. Pharm. Technol.* **2019**, *12*, 5865-5870, <http://doi.org/10.5958/0974-360X.2019.01017.5>.
 46. Nile, S.H.; Kim, D.H.; Nile, A.; Park, G.S.; Gansukh, E.; Kai, G. Probing the effect of quercetin 3-glucoside from *Dianthus superbus* L against influenza virus infection-*In vitro* and *in silico* biochemical and toxicological screening. *Food Chem. Toxicol.* **2020**, *135*, 110985, <https://doi.org/10.1016/j.fct.2019.110985>.
 47. Lopes, B.R.P.; da Costa, M.F.; Ribeiro, A.G.; da Silva, T.F.; Lima, C.S.; Caruso, I.P.; de Araujo, G.C.; Kubo, L.H.; Iacovelli, F.; Falconi, M.; Desideri, A.; de Oliveira, J.; Regasini, L.O.; de Souza, F.P.; Toledo, K.A. Quercetin pentaacetate inhibits *in vitro* human respiratory syncytial virus adhesion. *Virus Res.* **2020**, *276*, 197805, <https://doi.org/10.1016/j.virusres.2019.197805>.
 48. Aggarwal, M.; Leser, G.P.; Lamb, R.A. Repurposing Papaverine as an Antiviral Agent against Influenza Viruses and Paramyxoviruses. *J. Virol.* **2020**, *94*, 10-1128, <https://doi.org/10.1128/jvi.01888-19>.
 49. Khan, M.F.; Khan, M.A.; Khan, Z.A.; Ahamad, T.; Ansari, W.A. In-silico Study to Identify Dietary Molecules as Potential SARS-CoV-2 Agents. *Lett. Drug Des. Discov.* **2021**, *18*, 562-573, <https://doi.org/10.2174/1570180817999201209204153>.
 50. Gautret, P.; Lagier, J.-C.; Parola, P.; Hoanh, V.T.; Meddeb, L.; Mailhe, M.; Doudier, B.; Courjon, J.; Giordanengo, V.; Vieira, V.E.; Dupont, H.T.; Honoré, S.; Calson, P.; Chabrière, E.; La Scola, B.; Rolain, J.-M.; Brouqui, P.; Raoult, D. Hydroxychloroquine and azithromycin as a treatment of COVID-19: results of an open-label non-randomized clinical trial. *Int. J. Antimicrob. Agents* **2020**, *56*, 105949, <https://doi.org/10.1016/j.ijantimicag.2020.105949>.
 51. Liu, Y.; Yang, X.; Gan, J.; Chen, S.; Xiao, Z.-X.; Cao, Y. CB-Dock2: Improved protein–ligand blind docking by integrating cavity detection, docking and homologous template fitting. *Nucleic Acids Res.* **2022**, *50*, W159-W164, <https://doi.org/10.1093/nar/gkac394>.
 52. Wang, C.; Ye, X.; Ding, C.; Zhou, M.; Li, W.; Wang, Y.; You, Q.; Zong, S.; Peng, Q.; Duanmu, D.; Chen, H.; Sun, B.; Qiao, J. Two Resveratrol Oligomers Inhibit Cathepsin L Activity to Suppress SARS-CoV-2 Entry. *J. Agric. Food Chem.* **2023**, *71*, 5535-5546, <https://doi.org/10.1021/acs.jafc.2c07811>.
 53. Guérin, P.; Yahi, N.; Azzaz, F.; Chahinian, H.; Sabatier, J.-M.; Fantini, J. Structural Dynamics of the SARS-CoV-2 Spike Protein: A 2-Year Retrospective Analysis of SARS-CoV-2 Variants (from Alpha to Omicron) Reveals an Early Divergence between Conserved and Variable Epitopes. *Molecules* **2022**, *27*, 3851, <https://doi.org/10.3390/molecules27123851>.
 54. Thomsen, R.; Christensen, M.H. MolDock: A New Technique for High-Accuracy Molecular Docking. *J. Med. Chem.* **2006**, *49*, 3315-3321, <https://doi.org/10.1021/jm051197e>.
 55. Korb, O.; Stützle, T.; Exner, T.E. Empirical Scoring Functions for Advanced Protein–Ligand Docking with PLANTS. *J. Chem. Inf. Model.* **2009**, *49*, 84-96, <https://doi.org/10.1021/ci800298z>.
 56. Czaplewski, C.; Karczyńska, A.; Sieradzian, A.K.; Liwo, A. UNRES server for physics-based coarse-grained simulations and prediction of protein structure, dynamics and thermodynamics. *Nucleic Acids Res.* **2018**, *46*, W304-W309, <https://doi.org/10.1093/nar/gky328>.
 57. Al-Shuhaib, M.B.S.; Hashim, H.O.; Al-Shuhaib, J.M.B. Epicatechin is a promising novel inhibitor of SARS-CoV-2 entry by disrupting interactions between angiotensin-converting enzyme type 2 and the viral receptor binding domain: A computational/simulation study. *Comput. Biol. Med.* **2022**, *141*, 105155, <https://doi.org/10.1016/j.compbiomed.2021.105155>.
 58. Li, T.; Hendrix, E.; He, Y. Simple and Effective Conformational Sampling Strategy for Intrinsically Disordered Proteins Using the UNRES Web Server. *J. Phys. Chem. B* **2023**, *127*, 2177-2186, <https://doi.org/10.1021/acs.jpcc.2c08945>.

59. Shimoyama, H.; Yonezawa, Y. Atomistic detailed free-energy landscape of intrinsically disordered protein studied by multi-scale divide-and-conquer molecular dynamics simulation. *J. Comput. Chem.* **2021**, *42*, 19-26, <https://doi.org/10.1002/jcc.26429>.
60. Biskupek, I.; Sieradzan, A.; Czaplewski, C.; Liwo, A.; Lesner, A.; Giełdoń, A. Theoretical Investigation of the Coronavirus SARS-CoV-2 (COVID-19) Infection Mechanism and Selectivity. *Molecules* **2022**, *27*, 2080, <https://doi.org/10.3390/molecules27072080>.
61. Kachlishvili, K.; Maisuradze, G.G.; Martin, O.A.; Liwo, A.; Vila, J.A.; Scheraga, H.A. Accounting for a mirror-image conformation as a subtle effect in protein folding. *Proc. Natl. Acad. Sci.* **2014**, *111*, 8458-8463, <https://doi.org/10.1073/pnas.1407837111>.
62. Lokhande, K.B.; Pawar, S.V.; Madkaiker, S.; Nawani, N.; Venkateswara, S.K.; Ghosh, P. High throughput virtual screening and molecular dynamics simulation analysis of phytomolecules against BfmR of *Acinetobacter baumannii*: anti-virulent drug development campaign. *J. Biomol. Struct. Dyn.* **2022**, *41*, 2698-2712, <https://doi.org/10.1080/07391102.2022.2038271>.
63. Chen, T.-H.; Tsai, M.-J.; Chang, C.-S.; Xu, L.; Fu, Y.-S.; Weng, C.-F. The exploration of phytocompounds theoretically combats SARS-CoV-2 pandemic against virus entry, viral replication and immune evasion. *J. Infect. Public Health* **2023**, *16*, 42-54, <https://doi.org/10.1016/j.jiph.2022.11.022>.
64. Chaieb, K.; Kouidhi, B.; Hosawi, S.B.; Baothman, O.A.S.; Zamzami, M.A.; Altayeb, H.N. Computational screening of natural compounds as putative quorum sensing inhibitors targeting drug resistance bacteria: Molecular docking and molecular dynamics simulations. *Comput. Biol. Med.* **2022**, *145*, 105517, <https://doi.org/10.1016/j.compbiomed.2022.105517>.
65. Venkataraman, S. Plant Molecular Pharming and Plant-Derived Compounds towards Generation of Vaccines and Therapeutics against Coronaviruses. *Vaccines* **2022**, *10*, 1805, <https://doi.org/10.3390/vaccines10111805>.